EOS
EOS, TRANSACTIONS, AMERICAN GEOPHYSICAL UNION

VOLUME 87 NUMBER 7
14 FEBRUARY 2006
PAGES 73–84

# Satellite Data Give Snapshot of the 2005 Pakistan Earthquake

PAGES 73, 77

While it is well-known that the collision of the Indian subcontinent with the Eurasian continent forms the Himalayas, the real-time spatial crustal movement of these plates is difficult to observe. However, scientists can witness a part of this process of the formation of the Himalayas through an eye in space: synthetic aperture radar (SAR).

From the European Space Agency's Envisat, a satellite with SAR, the details of crustal deformation resulting from a major earthquake—a chance snapshot of the growth of the Himalayas—has been captured. Envisat's SAR has provided important data about the northern Pakistan earthquake (M7.6) of 8 October 2005, which occurred in the Kashmir region in the northwestern part of the Himalayas.

There are two important findings in this article. First, the earthquake occurred on pre-existing active faults. This means that surveying existing faults is important for estimating future earthquake hazards and risks. Second, the satellite data show the ruptured earthquake faults in detail, allowing relief planners to quickly simulate and estimate the seismically damaged areas and the extent of the damage for prompt rescue and relief operations.

The crustal deformation mapped with SAR data from Envisat revealed that the newly deformed area occupies a ~90-kilometer-long northwest-southeast trending strip extending from Balakot, Pakistan, southeast through Kashmir, the disputed areas between Pakistan and India. The heavily-damaged area north of Muzaffarabad within the Pakistani-controlled area of Kashmir has the maximum deformation, as observed by the satellite. There are known active faults stretching to the northwest and southeast near the epicenter, which reveal some uplift (on the northeastern side) and dextral (right-lateral) strike-slip activities.

BY S. FUJIWARA, M. TOBITA, H. P. SATO, S. OZAWA, H. UNE, M. KOARAI, H. NAKAI, M. FUJIWARA, H. YARAI, T. NISHIMURA, AND F. HAYASHI

The detected crustal deformation was along these active faults and all observations were consistent with previously known directions of past fault movements. Model calculations also showed that the faults slipped a maximum of about nine meters.

In addition, analysis using other high-resolution images from the Space Imaging, Inc. IKONOS satellite showed that landslides occurred along the active faults and were concentrated on the northeastern side.

### *Method and Analysis*

SAR measures ground geometry and the distance between the satellite and the ground surface with radar waves. By compiling several successive radar pulses from a source moving over a target, an image can be formed of that target that combines all the received echoes. In particular, interferometric synthetic aperture radar (InSAR) from space, which calculates the pixel-by-pixel phase differences between two SAR images generated at different times over the same location, has become a powerful tool to monitor deformation of the Earth's surface because the technique has high measurement accuracy (a few centimeters). However, Envisat's InSAR uses short-wavelength (5.6 centimeter, C-Band) radio waves, which makes it difficult to measure large deformation gradients or make measurements in precipitous terrain.

In this study, earthquake deformation was found by comparing InSAR and SAR images of the same region, one before the earthquake (17 September 2005) and one after (22 October 2005).

The Envisat data collected during this study are from descending acquisitions that result in an east-southeast line-of-sight (LOS) direction from the ground target to the satellite. The measured crustal deformation is the change in length along the radar LOS from the ground target to the SAR satellite. The components of displacement in each direction (north-south, east-west, and up-down) have not been directly determined. The result is an image that is not a traditional Cartesian map.

The largest observed displacement of the LOS displacement field of InSAR around the northern Pakistan earthquake damage area is ~30 centimeters of LOS movement toward the satellite. However, maps of displacement as calculated by InSAR were incoherent near the fault mainly because of the high deformation gradients resulting from the large displacement (approximately several meters): Because the measured phase is only modulo $2\pi$ rad (half of the wavelength), the phase in the high deformation gradients area changes too rapidly to count the phase cycles; in other words, undersampling occurs. Furthermore, strong seismic motion near the fault caused a loss of coherence over the damaged area.

Because InSAR cannot measure deformations in areas where deformation gradient is too large, the displacement fields of the two SAR amplitude images taken before and after the earthquake were measured using a sub-pixel-level offset estimation technique [*Tobita et al.*, 2001]. Its measurement accuracy is lower (~1 meter) than that of InSAR, but it succeeded in detecting this deformation that is impossible to measure with InSAR. Figure 1a is a combination map of the InSAR and the SAR offset field analyses, and it shows several-meter-scale crustal deformations extending in a strip. In addition, it shows that the heavily-damaged area north of Muzaffarabad experienced about five meters of deformation.

A fault model was constructed to simulate the surface displacement of Figure 1a. Using a buried fault model in a homogeneous elastic half-space, as formulated by *Okada* [1985], the model fault was divided into three rectangular faults on which slip is uniform. Optimal fault parameters were estimated using an iterative least squares method. The estimated parameters are listed in Table 1, and positions of each fault plane are shown in Figure 2. The calculated moment magnitude is 7.6, which matches the U.S. Geological Survey estimated magnitude.

### *Relationship Between Known Active Faults and Displacement*

Since most of the areas affected by the earthquake are in mountainous regions and access is prevented by landslides that have blocked the roads, ground survey is limited. At the moment, no exposed fault has been

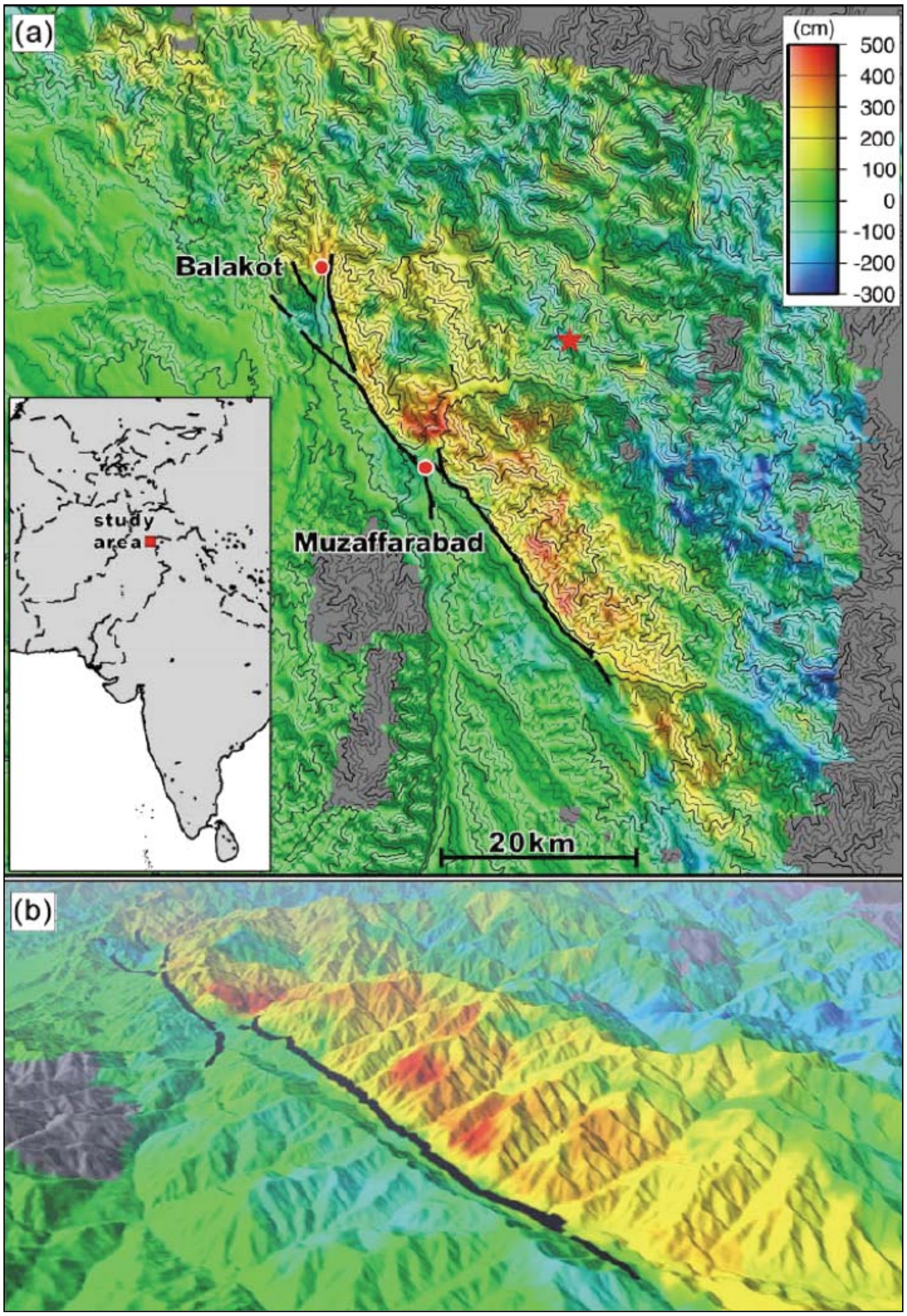


Fig.1 (a) Combined crustal deformation map superimposed on topography and the location of known active faults. Positive values indicate the movement of deformation, in centimeters, toward the SAR satellite in the LOS direction (upward and/or E-SE displacement). The red star shows the epicenter determined by the U.S. Geological Survey. The contour lines are every 250 meters (generated by the NASA Shuttle Radar Topography Mission). The black curves show the locations of active faults [Nakata et al., 1991] (see also http://www.fal.co.jp/geog_disaster/20051018_pakistan.html). (b) A bird's-eye view of crustal deformation and active faults (from the south).

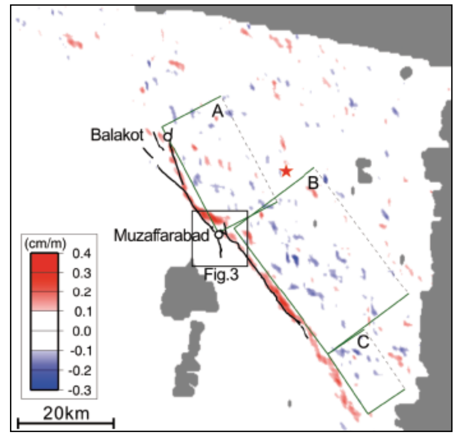


*Fig. 2. Surface displacement gradient map in the northeast-southwest direction. The black curves show the locations of active faults. Rectangles A, B, and C are the calculated fault positions, and dashed lines show the deeper side of each fault. The red star shows the epicenter determined by the U.S. Geological Survey.*

identified by ground survey or non-SAR measurement. Therefore, locating the earthquake faults by SAR data is important. The active faults in Figures 1, 2, and 3 were identified prior to the earthquake by interpreting aerial photographs, and were determined from geomorphologic analysis to be reverse dextral strike-slip faults with uplift on the northeastern side [*Nakata et al.,* 1991] (see also http://www.fal.co.jp/geog_disaster/20051018_pakistan.html).

The crustal deformation detected by this study is along these active faults, and both methods used were consistent in predicting the type of fault displacement that occurred. To estimate the position on the Earth's surface of the shallow side of the buried dipping faults, the surface displacement gradient [*Fujiwara et al.,* 2000] was calculated in the northeast-southwest direction (Figure 2) using data from the SAR deformation image shown in Figure 1a. The large gradient area clearly coincides with the known active faults. Therefore, this earthquake is considered to have been generated by movement on these preexisting active faults. Additionally, it shows that fault movement also occurred in the southern extension of these active faults.

Although there is a small discrepancy between the position of the shallow side of the simulated dipping faults and the area of the large displacement gradient, each extension of the buried shallow side to the surface generally agrees with the large gradient area. The rupture of northern fault plane 'A' approached closer to the surface than those of southern 'B' and 'C' (see Table 1).

The known active faults are divided in two fault groups, the Muzaffarabad fault (northwest of Muzaffarabad) and the Tanda fault (southeast of Muzaffarabad) [*Nakata et al.,* 1991]. These two faults run parallel near Muzaffarabad where the large gradient area in Figure 2 bends and transfers from the Muzaffarabad fault to the Tanda fault. Therefore, the model fault 'A' should be bending or split into several subfaults. Moreover, the maximum displacement is also found at 'A', so further research on the relationship between the bend of the large gradient area and the maximum displacement should be conducted.

The observations reported here show that earthquakes in the regional tectonic stress field tend to occur at the same preexisting faults and have formed the topography. The SAR analysis also shows that the topography and active faults have a close correlation to the displacement (see Figure 1). In other words, coseismic deformation mimics the topography [*Fujiwara et al.,* 2000]. It suggests that the known active faults are a result of accumulated fault movement over time.

## Distribution of Landslides

The distribution of landslides around Muzaffarabad was interpreted for the earthquake by comparing two one-meter-resolution IKONOS images, which were taken on

**Table 1. Simulated Fault Parameters**

| *Fault Position* | *Latitude, °N* | *Longitude, °E* | *Depth, km* | *Length, km* | *Width, km* | *Strike, deg* | *Dip, deg* | *Rake, deg* | *Slip, m* |
|---|---|---|---|---|---|---|---|---|---|
| A | 34.375 | 73.469 | 0.3 | 25 | 17 | 332 | 38 | 104 | 6.0 |
| B | 34.146 | 73.719 | 1.5 | 32 | 22 | 323 | 16 | 92 | 8.6 |
| C | 34.034 | 73.810 | 1.5 | 15 | 11 | 325 | 33 | 103 | 2.2 |

22 September 2002 (before the earthquake) and 9 October 2005 (after the earthquake). Those images are published on the Web (http://www.spaceimaging.com/gallery/asiaEQViewer.htm).

The area shown in Figure 3 is the central part of Figure 1a, around Muzaffarabad. The interpretation detected about 100 landslides, most of which occurred along the active faults concentrated on the uplift side (northeast). North and northwest of Muzaffarabad, large-scale landslides occurred. These landslides were located around a ~4-meter LOS earthquake displacement as seen by SAR; large-scale landslides are not identified southeast of Muzaffarabad, where LOS displacement as seen by SAR is only about one meter.

It is inferred that the large amount of uplift and/or strong seismic motion just over the fault triggered large-scale landslides. Geology in the landslide area is Tertiary limestone, calcareous sandstone, and shale. A partial field survey conducted for this study revealed that these types of rock were metamorphosed and weathered, but it could not be concluded that the large-scale landslides concentrate in a certain geological setting.

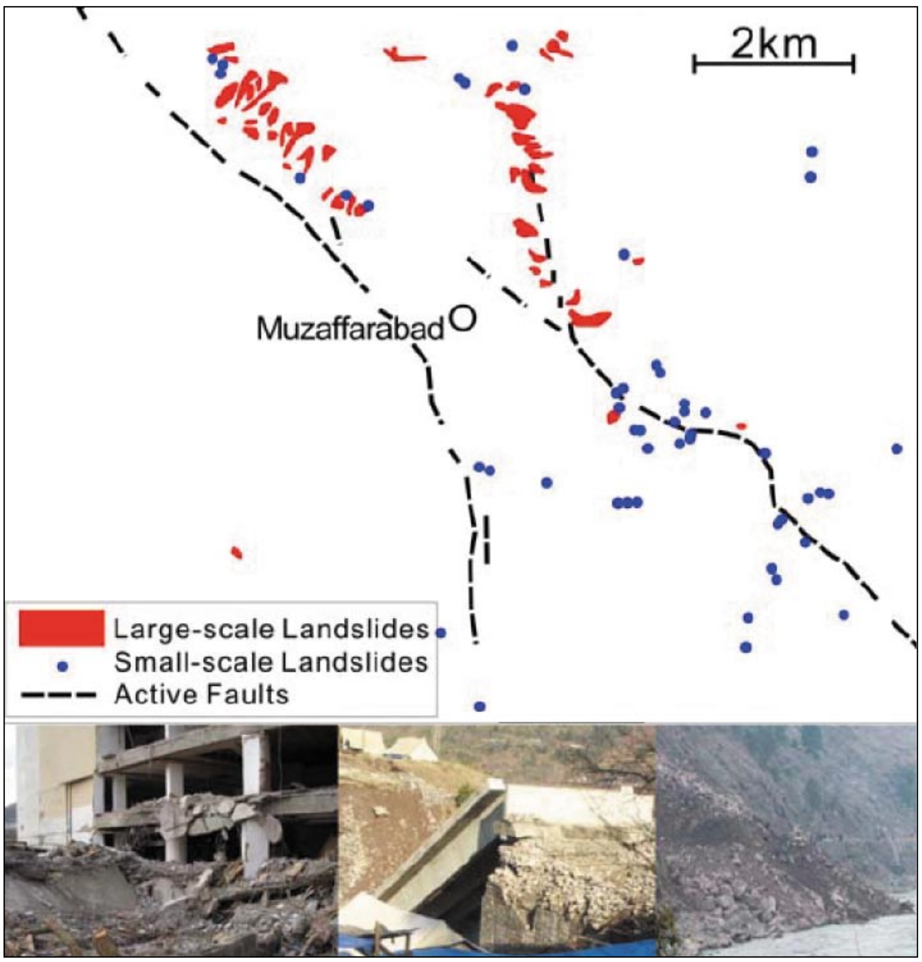


*Fig. 3. Distribution of landslides, interpreted using IKONOS imagery, and photographs of seismic damage around Muzaffarabad.*

## *Application to Disaster Mitigation*

For disaster mitigation, two lessons were learned from this study. First, the earthquake occurred on known preexisting active faults. Thus, surveys of existing faults are important for estimating future earthquake hazards and risk. Second, SAR observations can be used to estimate damaged areas for prompt rescue and relief operations because the SAR data show the earthquake faults in detail. From this, relief planners can simulate the seismic damage to effected areas. Perhaps if the displacement field was known immediately after the earthquake, relief operators could have expected that towns close to the earthquake faults such as Muzaffarabad and Balakot would suffer heavy damage.

These results show the importance of SAR data to the field of hazard and risk management. However, the number of SAR satellites is limited—only ESA's ERS-2 and Envisat, and Canada's RADARSAT-1 were in operation in 2005. However, the Japan Aerospace Exploration Agency launched the Advanced Land Observing Satellite (ALOS) on 24 January 2006. ALOS has an L-band SAR sensor, which generally has better coherence (higher signal to noise ratio) than C-band. RADARSAT-2 will be launched later this year.

## *References*

Fujiwara, S., T. Nishimura, M. Murakami, H. Nakagawa, M. Tobita, and P. A. Rosen (2000), 2.5-D surface deformation of M6.1 earthquake near Mt Iwate detected by SAR interferometry, *Geophys. Res. Lett.*, *27*(14), 2049–2052.

Nakata, T., H. Tsutsumi, S. H. Khan, and R. D. Lawrence (1991), Active faults of Pakistan, 141 pp., Res. Cent. for Reg. Geogr., Hiroshima Univ., Hiroshima, Japan.

Okada, Y. (1985), Surface deformation due to shear and tensile faults in a half-space, *Bull. Seismol. Soc. Am.*, *75*, 1135–1154.

Tobita, M., M. Murakami, H. Nakagawa, H. Yarai, S. Fujiwara, and P. A. Rosen (2001), 3-D surface deformation of the 2000 Usu eruption measured by matching of SAR images, *Geophys. Res. Lett.*, *28*(22), 4291–4294.

## *Author Information*

Satoshi Fujiwara, Mikio Tobita, Hiroshi P. Sato, Shinzaburo Ozawa, Hiroshi Une, Mamoru Koarai, Hiroyuki Nakai, Midori Fujiwara, Hiroshi Yarai, Takuya Nishimura, and Fumi Hayashi; E-mail: fujiwara@gsi.go.jp, Geographical Survey Institute, Tsukuba, Japan